Investigating Explosive and Material

Properties by Use of the Plate Dent Test

LOS ALAMOS SCIENTIFIC LABORATORY

Post Office Box 1663   Los Alamos. New Mexico 87545

This report was not edited by the Technical
Information staff.

ı

UNITED STATES
DEPARTMENT OF ENERGY
CONTRACT W-7405-ENG. 36

Investigating Explosive and Material
Properties by Use of the Plate Dent Test

George H. Pimbley
Allen L. Bowman
Wayne P. Fox
James D. Kershner
Charles L. Mader
Manuel J. Urizar

INVESTIGATING EXPLOSIVE AND MATERIAL PROPERTIES

BY USE OF THE PLATE DENT TEST

by

George H. Pimbley, Allen L. Bowman, Wayne P. Fox,
James D. Kershner, Charles L. Mader, and Manuel J. Urizar

ABSTRACT

The plate dent test is a fast, reliable, and inexpensive
way to estimate the relative performance and CJ pressures of
new explosives. In this report we describe a method whereby
the plate dent technique is used to estimate the yield strength
of a material. Yield strengths of steel, aluminum, beryllium,
lead, and Tuballoy are examined.

I. INTRODUCTION

An important parameter of an explosive is its CJ pressure. Unfortunately, this is also one of the most difficult explosive properties to measure accurately. The available methods require measurement of the free-surface velocities of metal plates driven by explosive charges using a smear camera technique.[1,2]

Historically, CJ pressure measurement has been associated with attempts to measure the ill-defined property called brisance. Brisance is vaguely the local shattering effect of an explosive. The notion is an old one, and attempts at measurement probably date back to the lead cylinder compression test of Hess in 1899 (see Refs. 3, p. 312; and 4). Other brisance tests are discussed in the literature (Refs. 3, p. 310; 5, and 6), but the test results did not correlate. More sensitivity to explosive load density was shown in some of the tests than in others. The same property may or may not have been measured in the various tests for brisance.

Then two papers by R. Becker[7,8] appeared which proposed that brisance be defined simply as the CJ pressure of the explosive. Because the historical meaning of the word "brisance" had implied more than mere CJ pressure (in varying and unknown degrees, effects resulting from charge size, impedance, detonation product isentropes, etc.), the older, intuitive ideas persisted. Gradually, Becker's definition was accepted.

In the early 1940s a brisance test was evolved that gave reasonable correlations with the CJ pressure data then available. This has become known as the plate dent test. Prominent developers were D. P. MacDougall and E. H. Eyster, then of the Explosive Research Laboratory in Bruceton, Pennsylvania, but, for

1

over 30 years since, of the Los Alamos Scientific Laboratory (LASL). The test was refined by L. C. Smith, M. J. Urizar, E. James, Jr., and J. B. Panowski, all of LASL.

Described briefly, the plate dent test calls for an explosive cylinder to be mounted vertically on a cold-rolled steel plate of given hardness. A detonator is fixed to the top of the explosive. The cylinder should be tall enough that an approximately steady detonation wave can develop in the cylinder after initiation. The steel plate should be sufficiently strong and massive that damage as a result of the explosion is confined to a dent, whose depth is not dependent upon distortions of the entire plate.

Plate dent tests are also conducted using aluminum alloy plates. In assessing explosives, steel or aluminum plate dent tests are used as references because these are the metals with adequately known material properties (Ref. 9, p. 277).

The plate dent test has been simulated numerically at LASL, using the 2DE code with elastic-plastic flow incorporated into the calculation. Experience indicated that the test might have uses other than the inference of CJ pressures; that is, the test might be turned around so that a known explosive could be used to study properties of a material by measurement of a dent.

A metal's yield strength is a property that often is not adequately known. By making plate dent experiments and using numerical simulation, correlations might be found between dent depth and the yield strength of a metal, using TNT or PBX 9404 as an explosive.

Section II of this report discusses the problem of finding explosive CJ pressures, using known materials and dent depths resulting from a plate dent test. Section III deals with the more speculative matter of finding the yield strength of a material, using a known explosive, together with plate dent data.

II. DETERMINATION OF EXPLOSIVE CJ PRESSURES BY USE OF THE PLATE DENT TEST

A. Experimental Technique

1. The Arrangement. The test explosive samples are cylindrical, and those of L. C. Smith (Ref. 10, p. 107) were 1.625 in. diameter and 8 in. long. Several of the 6-in.-square, 2-in.-thick steel plates are stacked, and the top plate is lightly greased for good coupling. The test charge is centered on the plate (Fig. 1), an adequate-sized booster is fastened on the charge, and the detonator is put in place.

2. Making the Measurement. The shot is fired and the dent is measured. Because irregularities often occur in the dent (Fig. 2), the apparatus shown in Fig. 3 is used to measure the dent. The outer ring provides support for the depth micrometer. If the ball bearing diameter is the same as the height of the ring, the micrometer reading is the depth.

Test reproducibility appears to depend upon the charge quality. According to Smith (Ref. 10, p. 108), values obtained for the solid explosive dent depths from five shots will usually agree to within 0.015 in. Sometimes an outlying observation, perhaps owing to a faulty plate or charge, will have to be rejected.

Smith cites his experience at LASL (Ref. 10, p. 108) in calibrating the test. Dent depths were obtained for pressed TNT charges with densities ranging from 1.58 to 1.64 g/cm^3. The individual shot data and the least-squares line are shown in Fig. 4. The average deviation of the points from the line is only 0.0031 in., although the dent depths were recorded only to the nearest 0.001 in.
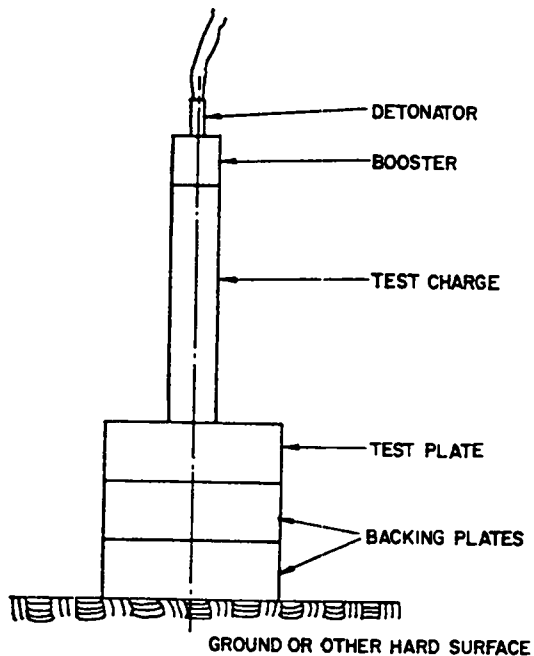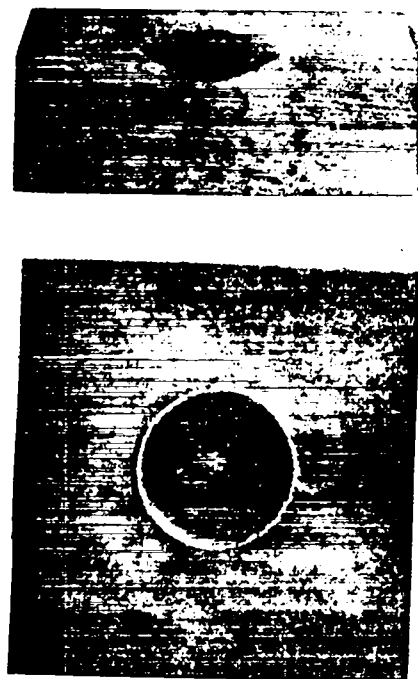
Fig. 1
Plate dent test configuration.

Fig. 2.
Photographs of the dent (about 0.435 in.
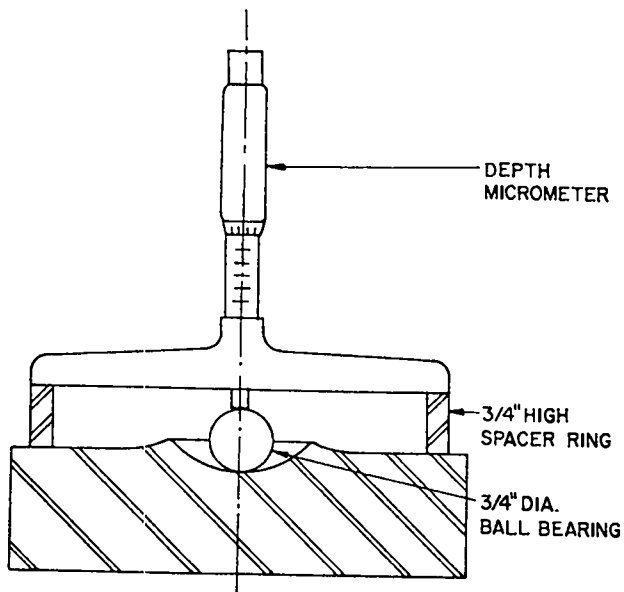deep) produced by a brisant explosive.

Fig. 3.
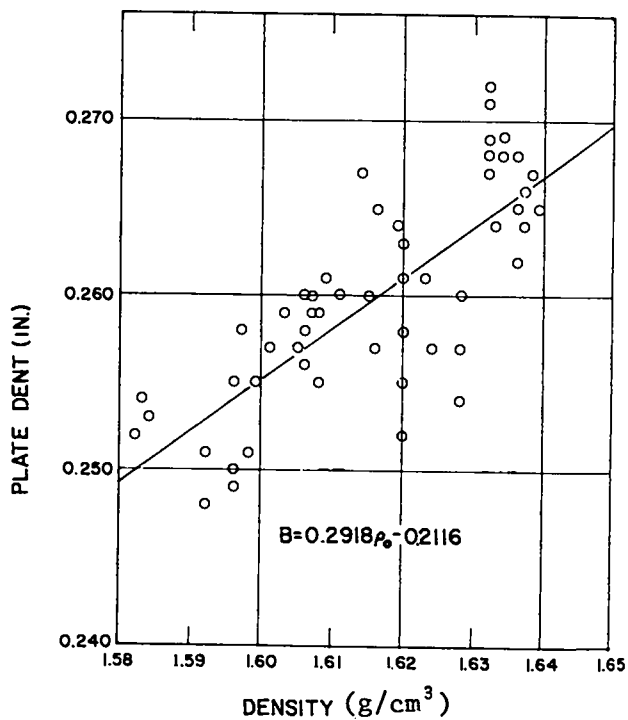Dent measurement apparatus.

$B = 0.2918 \rho_o - 0.2116$

Fig. 4.
Plate dent vs density in pressed TNT.

Undue significance ought not to be given a least-squares line, but the importance of controlling charge density effects is clear. A density change in pressed TNT of 0.01 g/cm³ produces a 0.003 in. change in dent depth, according to Fig. 4. Less complete results on other more powerful explosives lead to slightly higher deviations. Smith (Ref. 10, p. 109) used an overall compromise ratio of 0.004 in./0.01 g/cm³ in adjusting for density variations in LASL dent test results from several explosives.

       3.   Some Test Data. Table I shows data gathered by Smith in routine plate dent test application, with various explosives on steel plates. The densities in column 2 have been adjusted for fluctuation; the charge densities actually used often differed marginally from these. The pressures, velocities, and dents appearing in columns 3, 4, and 5 correspond directly with the densities given in column 2.

The first set of pressure measurements in Table I was obtained by A. W. Campbell, W. C. Davis, and B. G. Craig of LASL. The second set was obtained by W. E. Deal. The remaining CJ pressures were from the literature (Ref. 11, p. 840).

B.   The Inference of CJ Pressure

We infer now the relationship between explosive plate dents and detonation pressures, using Table I data and the least-squares method (Ref. 12, p. 211). In Fig. 5 the dent depth measurements (in cold-rolled steel) are plotted against CJ pressures in kilobars. The one outlying observation corresponding to the lead-loaded explosive was omitted. The regression line equation so determined is $B = 0.001097P + 0.0234$. The dent depth variable is called B in deference to the longstanding notion of Brisance.

We are more interested, however, in predicting CJ pressures from the plate dent experiment results than in predicting dent depths. The linear regression of P on B is more workable. When B is the independent variable and the least-squares method is applied, the equation for the least-squares line is $P = 847.7B$ (Ref. 10, p. 133). The pressures so computed and the differences from experimental values are given in Table I, columns 9 and 10.

The dent given by the lead-loaded composition RDX/Pb/Exon (19th entry in Table I) is more than twice the size that would be predicted by the detonation pressure. Evidently, the plate-denting value of an explosive can be increased spectacularly by adding lead. There are as yet no satisfying analytical explanations for this. The inclusion of such effects in the linear regression calculation seemed unjustified.

C.   Numerical Modeling of the Plate Dent Test for CJ Pressure

Because of insufficient realism in treating material properties, the usual Lagrangian or Eulerian codes available at LASL cannot describe the highly distorted flow taking place in dent formation. The recent inclusion of elastic-plastic flow in the LASL 2DE code (Ref. 9, pp. 353-404) allows the simulation of these effects (Ref. 9, pp. 293-298).

Material properties of the metal plate determine basically when the dent stops expanding in the test. If the plate lacked strength and were treated only hydrodynamically, the dent would expand indefinitely.

M. J. Urizar of LASL performed plate dent tests on thick blocks of aluminum alloy, reporting a 0.9-cm-deep, 3.70-cm-wide dent caused by a 2.54-cm-diam charge of TNT. The experiment was simulated numerically at LASL, using the BKW

4

TABLE I

PLATE DENT DATA

Explosive (Composition in Weight Percent)	ρ₀ (g/cm³)	P (kbar)	D (m/s)	Plate Denting Value Absolute (in.)	Relative (% of 1.63 g/cm³ TNT)	0.2582 ρ₀ D² (kbar)	Difference Calc-Exp.	447.7 B (kbar)	Difference Calc-Exp.
Nitromethane	1.133	139	6245	0.163	62	114	— 25	138	— 1
TNT	1.633	212	6945	0.265	100	203	— 9	225	+ 13
Composition A (91/9-RDX/Wax)	1.631	287	6370	0.322	122	295	+ 8	273	— 14
29.7/64.9/5.4 - HMX/NQ/Estane	1.712	301	6380	0.291	110	310	+ 9	247	— 54
Composition B (60.7/39.3 - RDX/TNT)	1.730	304	7980	0.340	129	284	— 20	288	— 16
86.4/13.6 - HMX/Estane	1.738	307	8360	0.345	131	313	+ 6	292	— 15
PETN	1.670	310	7985	0.386	146	275	— 35	327	+ 17
Cyclotol (77/23 - RDX/TNT)	1.754	320	8290	0.369	140	311	— 9	313	— 7
90/10 - HMX/Estane	1.767	324	8500	0.370	140	330	+ 6	314	— 10
93.4/6.6 - HMX/Estane	1.800	334	8670	0.394	149	350	+ 16	334	± 0
90/10 - RDX/Kel-F 3700	1.783	337	8370	0.393	149	323	— 14	333	— 4
85.6/9.2/5.2 - HMX/DATB/Estane	1.798	343	8575	0.404	153	341	— 2	342	— 1
65.7/26.4/7.9 - HMX/NQ/Kel-F 3700	1.815	346	8625	0.390	148	349	+ 3	331	— 15
85/15 - HMX/Viton	1.852	348	8430	0.402	152	340	— 8	341	— 7
94/3/3 - HMX/NC/CEF (PBX-9404)	1.840	372	8790	0.435	165	368	— 4	369	— 3
Cyclotol (75.2/24.8 - RDX/TNT)	1.200	124	6490	0.212	80	130	+ 6	180	+ 56
Baratol (76/24 - Barium Nitrate/TNT)	2.610	140	4925	0.127	48	163	+ 23	108	— 32
Nitromethane	1.133	145	6245	0.163	62	114	— 31	138	— 7
23.3/73.0/3.7 - RDX/Pb/Exon	4.606	148	5010	0.405	153	298	+ 150	343	+ 195
60.8/39.2 - TNT/DNT	1.579	178	6755	0.228	86	185	+ 8	193	+ 15
TNT	1.637	189	6950	0.266	101	204	+ 15	225	+ 36
93.9/3.8/2.3 - RDX/PS/DOP	1.713	286	8430	0.365	138	314	+ 28	309	+ 23
Composition B (64/36 - RDX/TNT)	1.714	290	7990	0.339	128	283	— 7	287	— 3
Cyclotol (77/23 - RDX/TNT)	1.743	312	8250	0.364	138	306	— 6	309	— 3
Octol (76.3/23.7 - HMX/TNT)	1.609	338	8450	0.396	150	334	— 4	3*6	— 2
RDX	1.767	338	8640	0.414	157	341	+ 3	351	+ 13
92/6/2 - HMX/Exon/CEF	1.837	344	8665	0.422	160	356	+ 12	358	+ 14
94/3/3 - HMX/NC/CEF (PBX 9404)	1.844	364	8800	0.437	166	369	+ 5	370	+ 6
Nitromethane	1.133	129		0.163	62				
TNT	1.59	202		0.252	95				
RDX	1.755	366		0.408	155				
Tritonal (80.9/19.1 - TNT/Al)	1.730			0.241	91				
38.7/29.5/31.8 - RDX/TNT/Al	1.864			0.266	101				
45.8/33.5/20.7 - RDX/TNT/Al	1.762			0.289	109				
Pentolite (54.7/45.3 - PETN/TNT)	1.655			0.309	117				
Tetryl	1.681			0.319	121				
RDX	1.537			0.323	122				
92/6/2 - RDX/PS/DOP	1.685			0.342	135				
HMX	1.730			0.397	150				

NOTES — Materials and abbreviations:
NQ . . . . . Nitroguanidine
NC . . . . . Nitrocellulose
DATB . . . Diaminotrinitrobenzene
Exon. Kel-F . See text
Estane . . . A B. F. Goodrich Company polyester-urethane resin
Viton A . . A duPont perfluoropropylene/vinylidine fluoride copolymer
CEF . . . . . tris (β-chloroethyl) phosphate
PS . . . . . Polystyrene
DOP . . . . . Dioctylphthalate

The explosives are grouped according to the source of the pressure measurements. From the top they are: GMX-8, GMX-6, and literature values (ref 11). Pressure data for the last group in the table were not available.

Nitromethane plate dent was determined at 30°C in 1/16" wall polystyrene tubes.
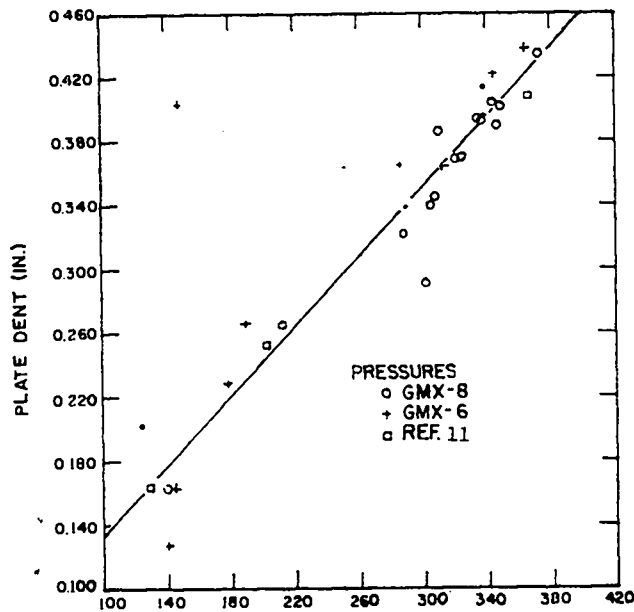
Fig. 5.
Plate dent vs CJ pressure.

equation of state (Ref. 9, pp. 412-418) and with the TNT burned using the CJ volume burn technique (Ref. 9, p. 316). An aluminum equation of state was used (Ref. 9, p. 165), with a previously determined 5.5 kbar yield strength and a shear modulus of 0.25 Mbar (Ref. 9, p. 277).

The calculated density contours are shown in Fig. 6 for a 1.27-cm-radius, 2.54-cm-long TNT charge interacting with the aluminum plate. The plan of the calculation is shown in Fig. 7. The cells are 0.1-cm-square. Prescribed boundary conditions are shown (Ref. 9, pp. 345-347). The explosive was initiated by detonating computationally the bottom 0.3 cm of TNT. Figure 6 shows the developing constant density contours (isopycnics) and the growing dent profile.

In Fig. 8 the same calculation is shown at 24 µs, but with the elastic-plastic option turned off. The material behaves hydrodynamically and the dent continues expanding. Figure 9 shows the axial vertical velocity of the explosive-metal interface as a function of time, both with and without treatment of the aluminum as an elastic-plastic material.

Similar calculations were performed with a steel plate. The yield strength used was 7.5 kbar and the shear modulus was 0.987 Mbar. Table II shows the comparative overall results for the two metals.

This numerical modeling has concerned conventional explosives having similar isentrope slopes near the CJ pressure. The major differences seem to be functions of the peak detonation pressure. The observed correlation of plate dent depth with CJ pressure is probably a consequence of the similar equation of state of the detonation products, down to about 10 kbar.

The unique behavior of the detonation products' equation of state of lead-loaded explosives may help to explain the failure of the dent depth to correlate with the CJ pressures.

The ability to reproduce observed plate dents numerically will greatly facilitate our attempts to describe explosives and materials. It may give the necessary insight for making improvements.

III. FINDING THE YIELD STRENGTH OF A MATERIAL DENTED WITH A KNOWN EXPLOSIVE

A. The Concept

In Sec. II the discussion centered on the use of dented plates of a known material (for example, aluminum or steel) to assess an important explosive parameter. Now we inquire whether we can assess an otherwise hard-to-measure property of a material, using the plate dent test and a well-known explosive (for example, TNT or PBX 9404).

The material property to be assessed is the yield strength Y_0. The yield strength of a material is a function of the strain rate. When the strain rates are low, laboratory apparatus has been used to determine the function. At high strain rates that might be caused by explosives, very little is known except for aluminum, steel, and a few other metals. If plate dents can be used to assess yield strength at high strain rates, we may be able to examine the yield strengths of materials such as Tuballoy.

If the plan is to be implemented, some type of correlation or other relationship should be established between plate dent depth and the plate material yield strength. By necessity, the approach is computational. Since yield strength is not at our disposal as an experimental independent variable, we cannot find a relationship between Y_0 and dent depth by experiment. However, in using the LASL 2DE code, Y_0 is an input item, adjustable at will (Ref. 9, p. 334).
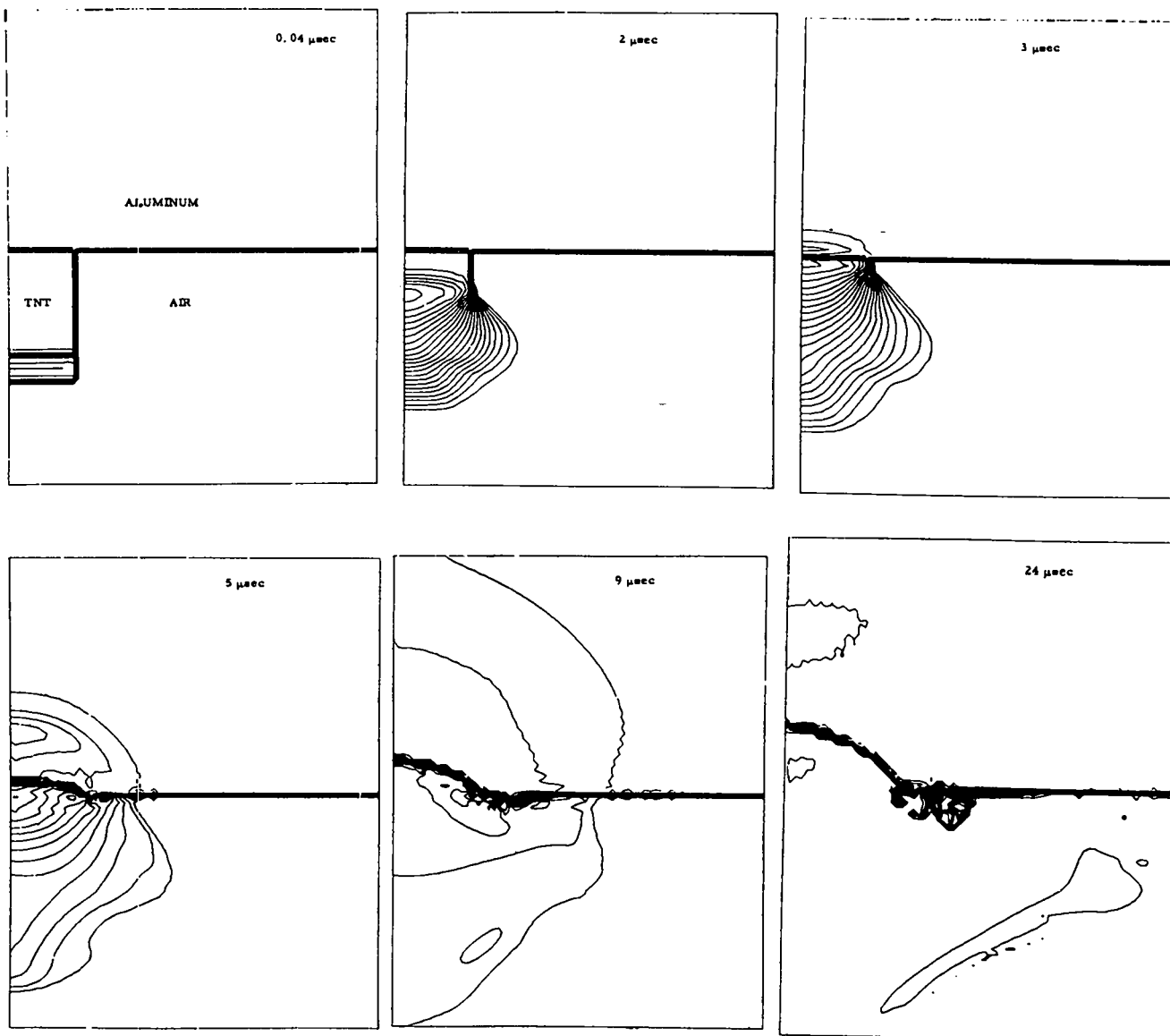
6

Fig. 6.

Density contours of 0.1 cm^3/g for 1.27-cm-radius, 2.54-cm-long TNT cylinder interacting with an aluminum plate. The bottom boundary is 7 cm long and the height is 9 cm.

TABLE II

EXPERIMENTAL AND CALCULATED PLATE DENTS

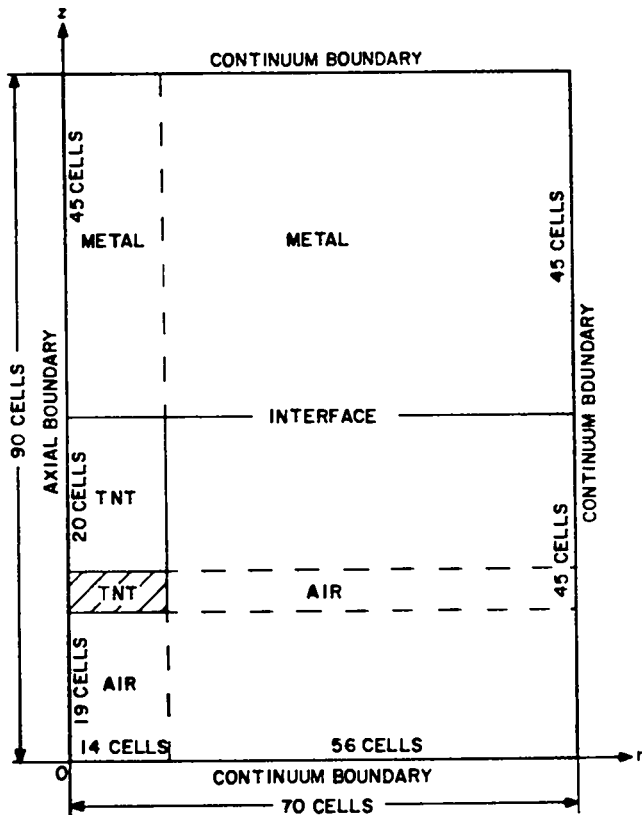| Diameter (cm)	Explosive	Metal	Experimental Plate Dent (cm)	Calculated Plate Dent (cm)
2.54	TNT	Dural	0.90	0.95
2.54	PBX 9404	Dural	1.66	1.70
4.13	TNT	Steel	0.67	0.75
4.13	PBX 9404	Steel	1.12	1.20

Fig. 7.
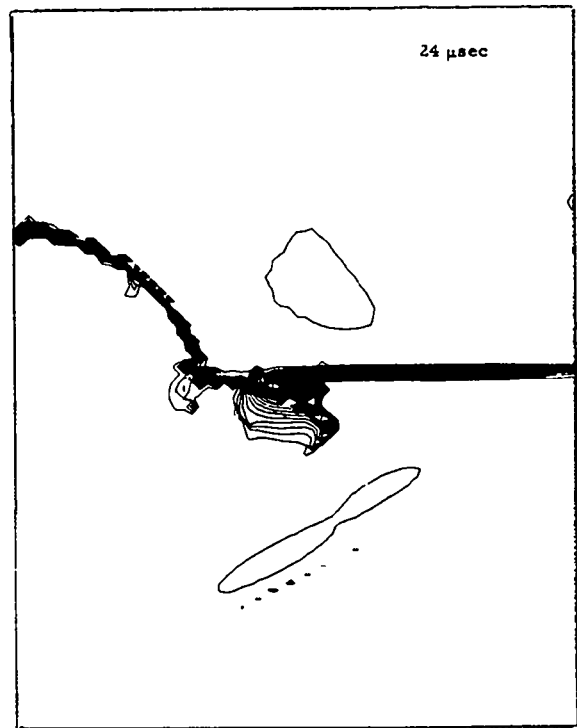A 2DE calculation plan for the aluminum and steel plate dent test.

Fig. 8.
Density contours at 24 µs for the same calculation as Fig. 6 but with aluminum treated as a fluid.
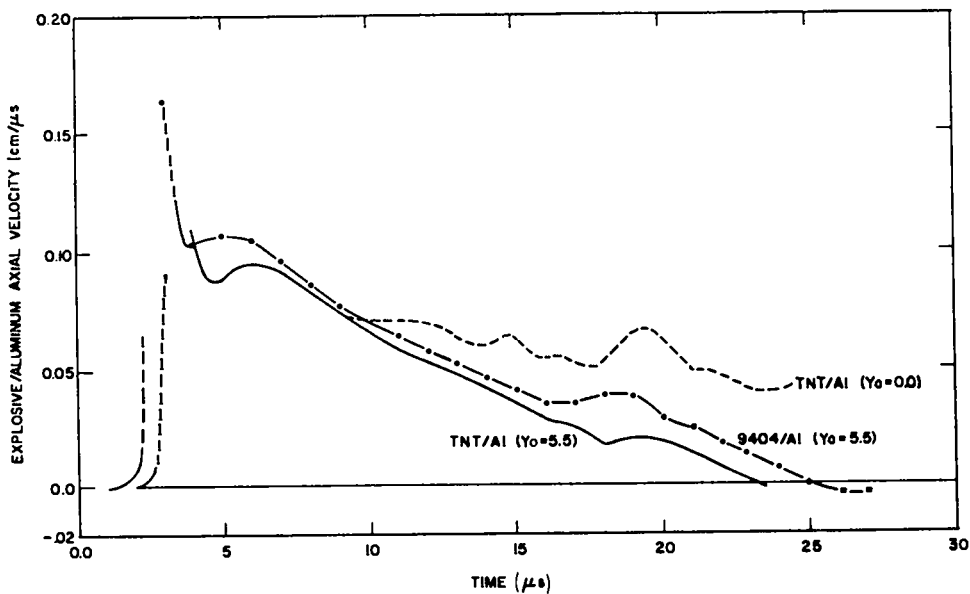

Fig. 9.
Velocity as a function of time in the axial explosive-aluminum interface for TNT and PBX 9404. Also shown is the TNT-aluminum interface velocity for fluid aluminum.

8

The intention, therefore, is to compute the dent depth of a hypothetical numerically modeled plate dent experiment. If it is available, we should first use an accepted yield strength value of the material in the computation. Next, several "yield strengths" would be chosen in a cluster about this accepted Y_0, the computation would be made, and the resulting numerically determined "dents" would be recorded. Thus we should obtain numerically a local function of dent depth vs. Y_0, anchored to the accepted experimental value in the middle.

We should hope that, with enough iterations of the procedure on different materials and known explosives, functional dependencies between Y_0 and dent depth could be predicted. Ultimately, we should hope to learn yield strengths merely by performing plate dent experiments.

Except for aluminum and steel, too little is known about yield strengths in the high-strain region to anchor the relationship to experimental values. Nevertheless, we proceed to use the method to obtain a functional dependence, Y_0 vs. dent depth, confined to probable ranges in which it is believed experimental yield strengths would lie. These relationships can then be used, with experimental dent depths of previously untested materials, to find some useful yield strength estimates.

B.   Numerical Modeling of the Inverse Plate Dent Experiment

We have already discussed plate dent computations for two well-known materials, aluminum and steel. Now we discuss the modeling of three materials with properties that are not as well known--beryllium, lead, and Tuballoy. Two well-known explosives, TNT and PBX 9404, were incorporated in the modeling.

1.   TNT on Beryllium.   The calculation plan is shown in Fig. 10. The dimensions are given for a cylindrical column of TNT, with initiator (shaded), which is shot computationally into a beryllium plate with dimensions as shown. The remainder of the problem rectangle in Fig. 10 consists of air. The problem boundary conditions are also indicated in Fig. 10 (Ref. 9, p. 345). A mesh is overlaid, with 40 cells in the R-direction, 70 cells in the Z-direction, and a 0.05-cm mesh. Cylindrical symmetric geometry is used, with the left boundary as the axis of symmetry.

The standard LASL HOM equations of state are used for the air, TNT, and beryllium, and the explosive is consumed using the CJ volume burn technique (Ref. 9, p. 316).

Three values are chosen for the beryllium yield strength Y_0--10, 18, and 25 kbar. The shear modulus is fixed at 1.615 Mbar.

To show graphically how the calculation proceeded, we present the successive density contours for $Y_0 = 25$ kbar in Fig. 11. Comparing Figs. 11c and 11d, the interface appears to have reached a steady state after 4 μs. The computational dent depth is determined by subtracting the z-coordinate of the undisturbed interface (Fig. 11a) along the axis of symmetry (left boundary) from the corresponding z-coordinate of the steady state dent (Fig. 11d). The actual data are used for this simple dent calculation, but the accuracy available in the calculation is no better than ± 0.04 cm.

The complete computational results for beryllium are summarized in Table III.

Table III also shows the experimental dent value obtained by subjecting a beryllium sample to the explosive impact of TNT, and the results are shown in

TABLE III

Y_0 vs DENT DEPTH – BERYLLIUM

EXPERIMENTAL DEPTH ≈ 0.241 cm

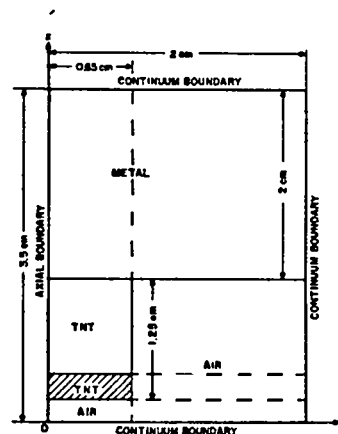| Y_0 (kbar)	Dent Depth (cm)
10	0.45 ± 0.04
18	0.33 ± 0.04
25	0.29 ± 0.04

Fig. 10.
A calculation plan for the TNT on beryllium plate dent calculation.

Fig. 12. The experimental dent value given in Table III is adjusted to take into account the dimensional disparities between the experiment and the measurements shown in Fig. 10 for the actual calculation.

As plotted in Fig. 13, a straight line may not be a bad fit for the data in Table III. The slope is about -104 kbar/cm. Using the experimental value (0.241 cm) of the dent, we estimate that Y_0 ∿ 29.5 kbar.

Evidently, the only way to improve the yield strength estimate would be to perform more 2DE calculations so as to base the straight line of Fig. 13 on more points, enough to use the least squares method (Ref. 12, p. 211). Preferably, the computed plate dent depths should surround the experimental value. Then, we could interpolate the data linearly and more believably, instead of having to extrapolate the data as was done in Fig. 13 to get the estimated Y_0 ≈ 29.5 kbar. Interpolation is innately a more stable process than extrapolation.

2. PBX 9404 on Beryllium. The calculations were expected to be similar. An experimental dent depth of 0.378 cm had been obtained. Figure 14a shows the experimental arrangement, and Fig. 14b shows the dent that resulted.

In the calculations, by searching a prognosticated region of possible yield strengths, a computed 0.37-cm dent depth was obtained at Y_0 = 25. Evidently, the Y_0-vs-dent-depth function for PBX 9404 on beryllium is serviceable for assessing yield strength at high strain rate levels. This yield strength was less than that obtained with TNT on beryllium but is well within the expected accuracy of the calculations. The yield strength inferred from the experiments is 27 ± 4 kbar.

LASL Beryllium plate impact experiments gave yield strengths varying from 1.5 to 15 kbar. This is much smaller than values we have found from plate denting. Beryllium is a peculiar material, in its anisotropic polycrystalline nature and its effect on yield strength, which were described by R. E. Swanson (Ref. 13, p. 2).

Note that in the plate dent experiment, the plates are ruptured internally near the dent (as is often observed if a tested plate is sectioned). Energy may be dissipated in this and other ways.

3. TNT on Lead. As we moved up the periodic table, lead was deemed to be an interesting material for yield strength assessment by plate denting. Lead

10
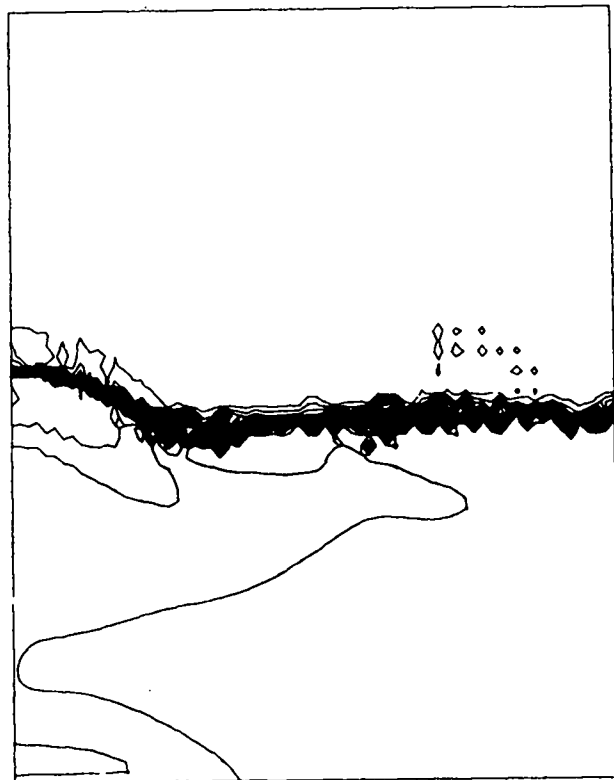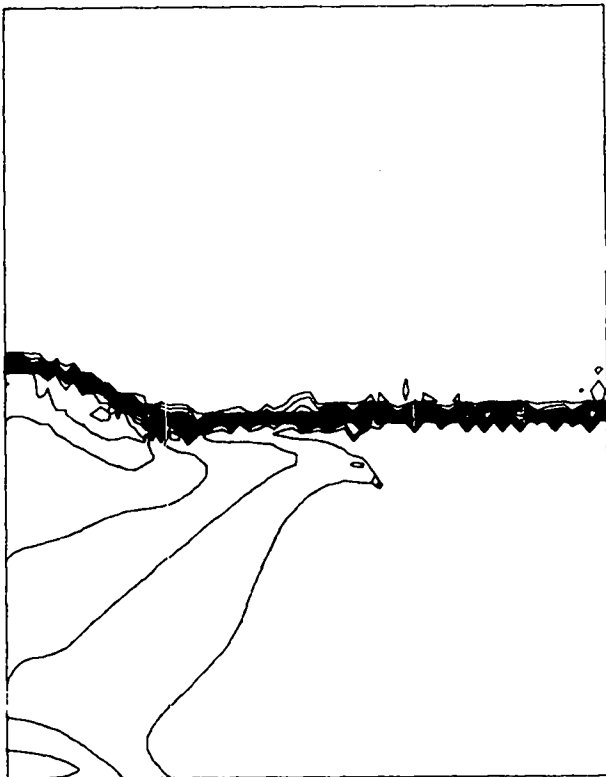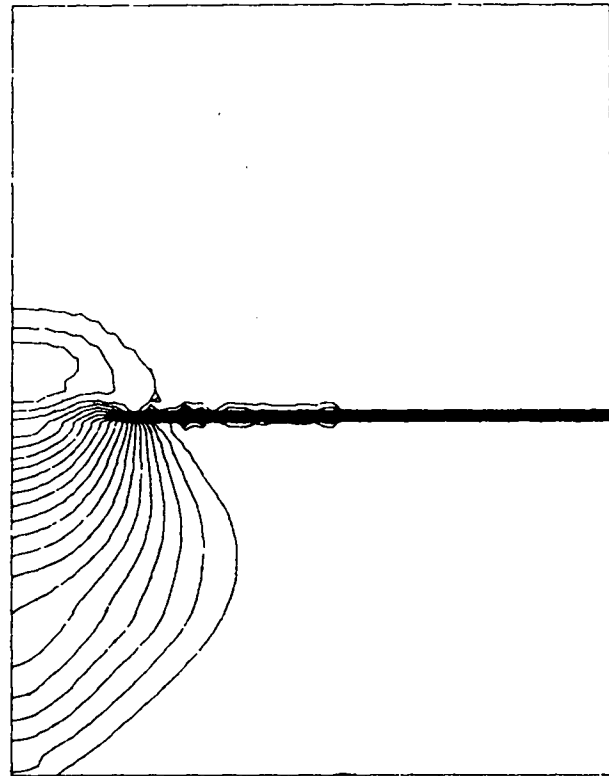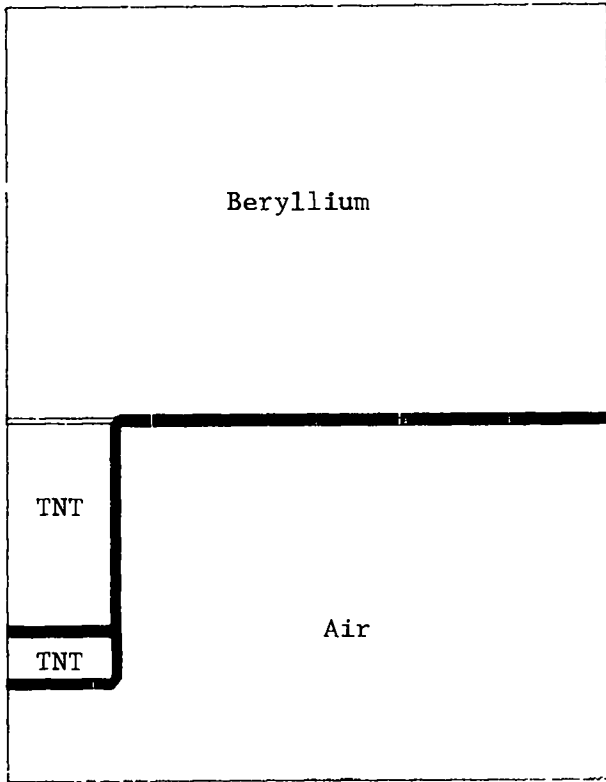
Fig. 11.
Density contours of 0.1 cm³/g for a 0.65-cm-radius, 1.25-cm-long cylinder of TNT
interacting with a beryllium plate. The bottom boundary is 2 cm long and the
height is 3.5 cm.
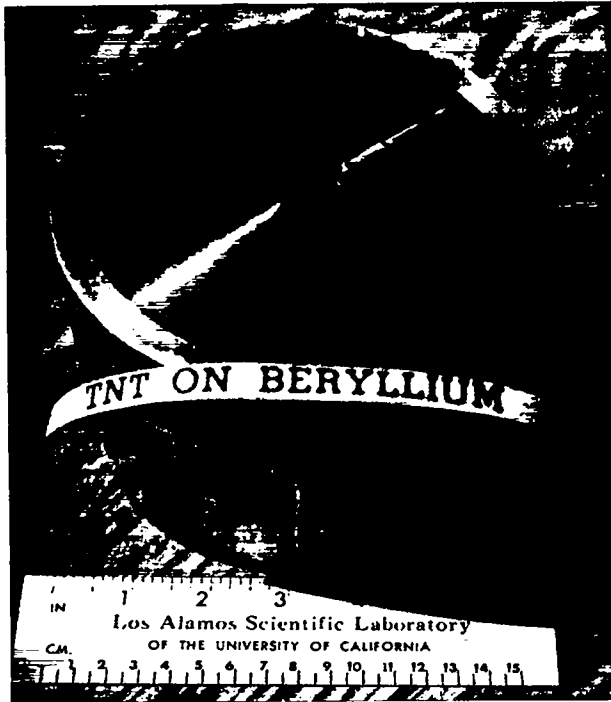
Fig. 12.
Beryllium sample dented with TNT.
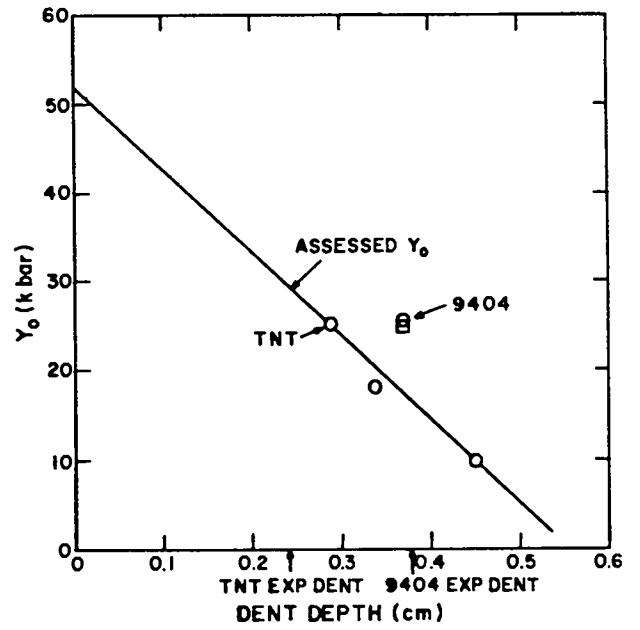
Fig. 13.
The yield strength Y_0 for beryllium assessed by use of the plate dent test.

Fig. 14a.
Pretest arrangement of PBX 9404 on beryllium.

Fig. 14b.
Beryllium sample dented with PBX 9404.

12

yield strengths are suspected to be comparatively low but are not well known. Lead plates have been subjected to LASL plate dent tests.

The calculation for TNT on lead was prepared using the plan shown in Fig. 10. Existing LASL HOM equations of state for air, TNT, and lead were employed, and again the CJ volume technique was used in burning the TNT (Ref. 9, p. 316). The calculation was performed using yield strengths of 2, 3, and 4 kbar, respectively. The shear modulus was fixed at 0.080/Mbar.

The computer runs with lead gave the results shown in Table IV. The calculations justified only the confidence intervals indicated in Table IV. As shown in Fig. 15, with this amount of confidence we can extrapolate linearly to obtain a yield strength estimate of about 0.1 kbar using the experimental dent depth value of 1.0514 cm. We are using the confidence widths to project a straight line giving a nonnegative Y_0 value. Possibly, with lead we are on the nonlinear portion of the theoretical Y_0-vs-dent-depth function that we are trying to investigate. Perhaps it is wrong to extrapolate linearly, but we have no criteria for a nonlinear extrapolation. We think that at zero yield strength the dent must expand indefinitely and that theoretically the depth should be infinite, although this does not help in practical estimates.

Methods of using the 2DE code should be refined and the resolution improved so that accurate computed data can be produced in the neighborhood of the experimental dent for lead, which is the lower part of the graph in Fig. 15.

    4.   TNT on Tuballoy.   Here, there existed an experimental dent depth value of 0.096 cm. The actual experimental arrangement and the actual physical dent are shown in Figs. 16a and 16b. Tuballoy, in contrast to beryllium and lead, does not dent easily. ·A previously used value of Y_0, 8 kbar, was chosen. The calculation then gave a 0.10-cm computed dent depth. The Y_0-vs-dent-depth functional relationship for Tuballoy seems to leave much to be desired however, as the next section shows.

    5.   PBX 9404 on Tuballoy.   A 0.185-cm experimental dent depth value was obtained in this case. Three calculations were made with the LASL HOM equation of state for Tuballoy and the Forest Fire burn technique. The shear modulus was 0.865 Mbar. The results are given in Table V.

This calculation does not appear to lend itself well to the finding of yield strengths Y_0 from computed dent depths, using the experimental dent depth (as was successful in the case of beryllium). Behind the difficulty is the need for greater spatial resolution in the calculation and, accordingly, a greatly refined mesh. The current mesh is as fine as can be contained conveniently in the CDC-7600 memory.

<div align="center">

TABLE IV

Y_0 vs   DENT DEPTH - LEAD

EXPERIMENTAL DEPTH $\approx$ 1.0514 cm

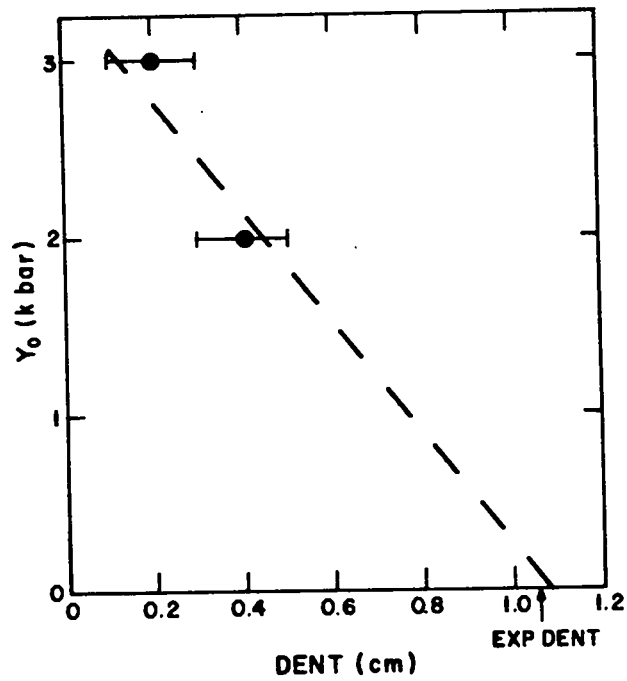| Y_0 (kbar)	Dent Depth (cm)
2	0.40 ± 0.10
3	0.21 ± 0.10
4	No trustworthy figure

</div>

Fig. 15.
The lead yield strength Y_0 assessed
by a plate dent test.
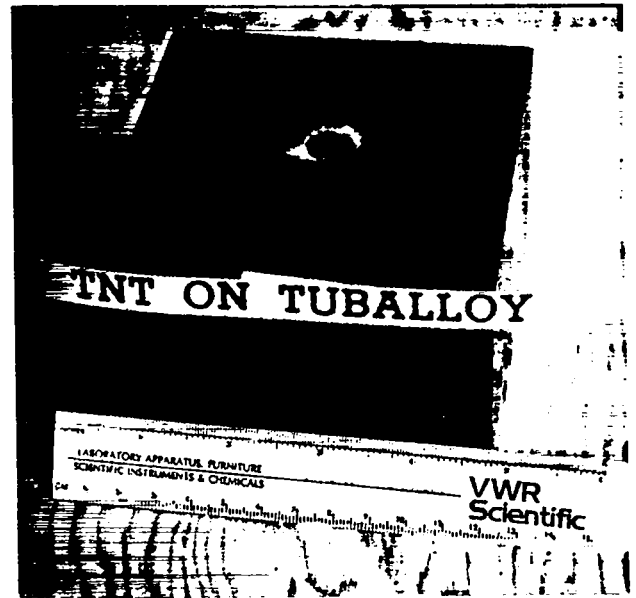

Fig. 16a.
Pretest assembly of TNT on Tuballoy.

Fig. 16b.
Tuballoy sample dented by TNT.

14

TABLE V

Y_0 vs DENT DEPTH - TUBALLOY

EXPERIMENTAL DEPTH $\approx$ 0.185 cm

Y_0 (kbar)	Dent Depth (cm)
8 (low resolution)	0.20 ± 0.04
8 (high resolution)	0.19 ± 0.02
5 (low resolution)	0.20 ± 0.04

6. __Interface Velocities.__ The metal-explosive interface velocity was plotted on the symmetry axis for the dent computations relative to the TNT-lead interface with Y_0 = 2 kbar (Fig. 17), the TNT-tuballoy interface with Y_0 = 8 kbar (Fig. 18), and the PBX 9404-Tuballoy interface with Y_0 = 8 kbar (Fig. 18). These can be compared with the axial velocity plots in Fig. 9 of the TNT-Al interface and the PBX 9404-Al interface.

IV. SUMMARY

Using a familiar plate material such as steel, the plate dent test is a well-established procedure for assessing CJ pressures of new explosives. The test is fast, reliable, and inexpensive. Efforts to model this test numerically, using the LASL Eulerian 2DE code, have also been satisfactory. Experimentally observed plate dent values have been well-approximated computationally using previously measured material properties. The resulting pressure, density, energy, and velocity contours, plotted against the time, indicate what happens internally to the plate during the test.

The inverse problem is that of taking a metallic material whose properties it is desired to determine, fabricating a plate, and then denting this plate with a familiar explosive to estimate parameters of the material.

We have tried to determine the plate material yield strength Y_0 at high strain rates. The approach has to be computational, because yield strength is not an available experimental independent variable to correlate with dent depth observations. Although some success can be claimed in using plate dents to estimate yield strengths in the more common materials, and even with beryllium, problems were encountered with lead because the experimental dents may lie in a nonlinear portion of a Y_0 vs. dent depth curve.

Finding yield strengths for high-density materials such as Tuballoy would be interesting. For such very dense metals, however, the required computational mesh refinement taxes the existing memory space in the CDC 7600 computer. The calculations indicate that very dense materials dent so slightly that they are not very suitable for plate dent testing. The data that result cannot be used to determine interesting material properties because the yield strength is such an insensitive function of the plate dent depth.

The previously used yield strengths for Tuballoy (in the range of 4-8 kbar) are consistent with the results of plate denting. On the other hand, the 27 kbar
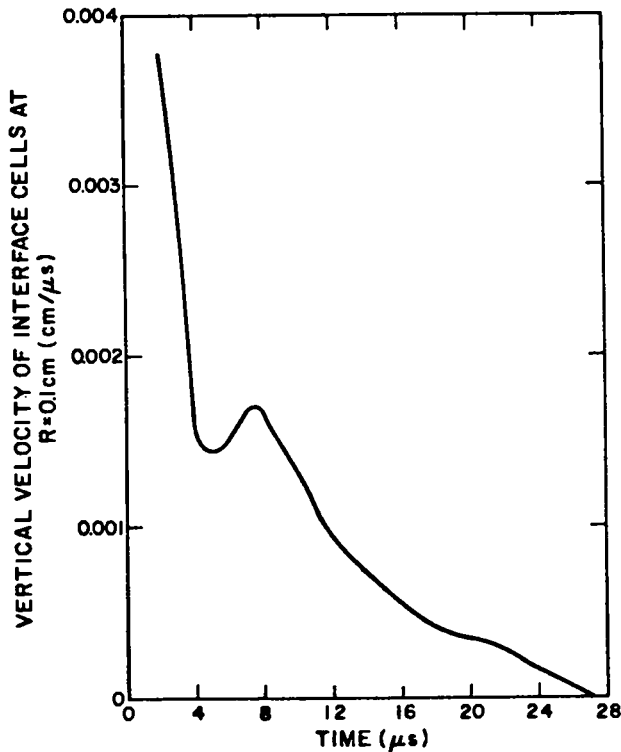
Fig. 17.
Axial velocity (cm/μs) of a lead dent interface shocked by TNT.
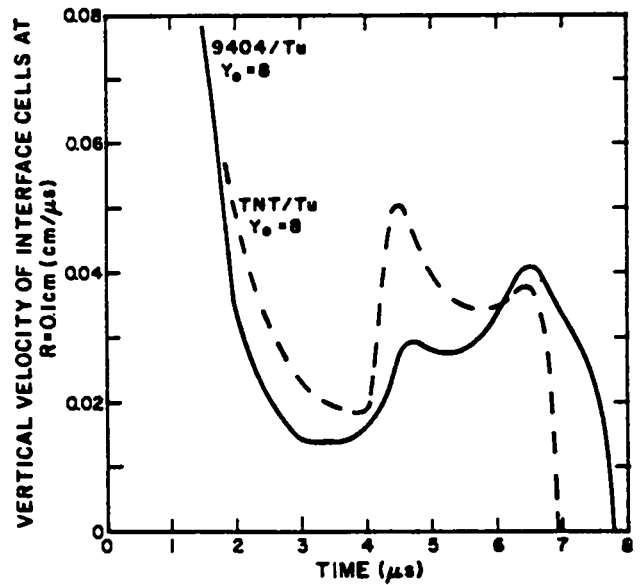
Fig. 18.
Axial velocity (cm/μs) of a Tuballoy dent interface shocked by TNT and PBX 9404.

beryllium yield strength, obtained herein by plate dent estimation, is considerably larger than yield strengths estimated previously from plate impact experiments. The characterization of polycrystalline beryllium needs additional study.

APPENDIX A

SOUND SPEEDS USED TO ESTIMATE SHEAR MODULUS

Material	Density, (g/cm^3)	Bulk Sound Speed	Long Sound Speed	Shear Modulus*
Aluminum	2.785	0.535	0.64	0.25
Steel	7.917	0.458	0.621	0.987
Lead	11.34	0.2028	0.225	0.0801
Beryllium	1.845	0.7975	1.3417	1.615
Tuballoy	18.98	0.254	0.254	0.865

* Calculated from $\rho_0 C_L^2 = \rho_0 C_B^2 + \frac{4}{3}\mu$.

16

The HOM equation of state is used to solve for pressure P and temperature T in a cell, with specific volume V and specific internal energy I as input. The shock velocity U_s and the particle velocity U_p are related by

$$U_s = C + SU_p \quad .$$

The equations for a solid are

$$P_H = c^2(V_0 - V)/[V_0 - S(V_0 - V)]^2$$

$$X = \ell n \, V$$

$$\ell n \, T_H = F + GX + HX^2 + IX^3 + JX^4$$

$$I_H = (1/2)P_H(V_0 - V)$$

$$P = (\gamma/V)(I - I_H) + P_H$$

$$T = (I - I_H)(23\,890)/C_V + T_H \quad .$$

The equations for a gas are

$$X = \ell n \, V$$

$$Y = \ell n \, P_i$$

$$Y = A + BX + CX^2 + DX^3 + EX^4$$

$$\ell n \, I_i = K + LY + MY^2 + NY^3 + OY^4$$

$$I_i = I_i - Z$$

$$\ell n \, T_i = Q + RX + SX^2 + TX^3 + UX^4$$

$$-1/\beta = R + 2SX + 3TX^2 + 4UX^3$$

$$P = [1/(\beta V)](I - I_i) + P_i$$

$$T = (I - I_i)(23\,890)/C_V' + T_i \quad .$$

The solution for a cell with more than one component is based on combinations of these equations.[9,15]

The equation-of-state parameters used in this study are tabulated in Table B-I. The units are volume (cm^3/g), energy ($Mbar-cm^3/g$), pressure (Mbar), temperature (K), velocity ($cm/\mu s$), and heat capacity (cal/g-K).

TABLE B-I

EQUATION OF STATE PARAMETERS

AIR

A	$-4.50602542688E+00$	D	$-1.58521895338E-06$
B	$-1.27546110628E+00$	Q	$8.22644581441E+00$
C	$-3.74276600292E-03$	R	$-2.51525130950E-01$
D	$1.23929236747E-02$	S	$-1.34446940047E-02$
E	$-2.07694122929E-03$	T	$1.40871016422E-02$
K	$-1.62655447438E+00$	U	$-2.18132189985E-03$
L	$9.05283146618E-02$	c'_v	$5.00000000000E-01$
M	$2.69004997726E-03$	Z	$1.00000000000E-01$
N	$-5.43583122192E-05$	ν_0	$8.65224000000E+02$

TNT

C	$2.71500000000E-01$	D	$6.04976925160E-02$
S	$2.57600000000E+00$	E	$-1.93025884483E-02$
F	$-8.66618495552E+00$	K	$-1.51924169032E+00$
G	$-5.83137822089E+01$	L	$5.30437118647E-01$
H	$-6.97163410850E+01$	M	$9.55633819122E-02$
I	$-8.20099102783E+00$	N	$9.09410350651E-03$
J	$2.07195569008E+01$	O	$3.44453952045E-04$
γ	$6.74700000000E-01$	Q	$7.57709458042E+00$
c_v	$4.00000000000E-01$	R	$-4.38746292676E-01$
ν_0	$6.09756097561E-01$	S	$9.22960569941E-02$
α	$0.$	T	$2.36679650544E-03$
A	$-3.66524588562E+00$	U	$-3.24343716606E-03$
B	$-2.46714261610E+00$	c'_v	$5.00000000000E-01$
C	$2.28461573300E-01$	Z	$1.00000000000E-01$

PBX 9404

C	$2.42300000000E-01$	D	$1.39083578508E-02$
S	$1.88300000000E+00$	E	$-1.13963024075E-02$
F	$-9.04187222042E+00$	K	$-1.61913041133E+00$
G	$-7.13185252435E+01$	L	$5.21518534192E-01$
H	$-1.25204979360E+02$	M	$6.77506594107E-02$
I	$-9.20424177603E+01$	N	$4.26524264691E-03$
J	$-2.21893825727E+01$	O	$1.04679999902E-04$
γ	$6.75000000000E-01$	Q	$7.36422919790E+00$
c_v	$4.00000000000E-01$	R	$-4.93658222389E-01$
ν_0	$5.42299349241E-01$	S	$2.92353060961E-02$
α	$5.00000000000E-05$	T	$3.30277402219E-02$
A	$-3.53906259964E+00$	U	$-1.14532498206E-02$
B	$-2.57737590393E+00$	c'_v	$5.00000000000E-01$
C	$2.60075423332E-01$	Z	$1.00000000000E-01$

ALUMINUM

c	$5.35000000000\mathrm{E}{-}01$	J	$-2.56423794962\mathrm{E}{+}01$
s	$1.35000000000\mathrm{E}{+}00$	γ	$1.70000000000\mathrm{E}{+}00$
F	$-2.07547507908\mathrm{E}{+}01$	c_v	$2.20000000000\mathrm{E}{-}01$
G	$-1.15617830366\mathrm{E}{+}02$	ν_0	$3.59066427290\mathrm{E}{-}01$
H	$-1.77762573069\mathrm{E}{+}02$	α	$2.40000000000\mathrm{E}{-}05$
I	$-1.14252754176\mathrm{E}{+}02$		

STEEL

c	$4.58000000000\mathrm{E}{-}01$	J	$-1.66391615983\mathrm{E}{+}02$
s	$1.51000000000\mathrm{E}{+}00$	γ	$2.00000000000\mathrm{E}{+}00$
F	$-3.82382587453\mathrm{E}{+}03$	c_v	$1.07000000000\mathrm{E}{-}01$
G	$-7.03211954024\mathrm{E}{+}03$	ν_0	$1.26310471100\mathrm{E}{-}01$
H	$-4.82670213890\mathrm{E}{+}03$	α	$1.17000000000\mathrm{E}{-}05$
I	$-1.46678402118\mathrm{E}{+}03$		

TUBALLOY

c	$2.54000000000\mathrm{E}{-}01$	J	$7.18306835194\mathrm{E}{+}00$
s	$1.50000000000\mathrm{E}{+}00$	γ	$2.00000000000\mathrm{E}{+}00$
F	$1.70969943945\mathrm{E}{+}01$	c_v	$2.76000000000\mathrm{E}{-}02$
G	$3.22821567236\mathrm{E}{+}01$	ν_0	$5.28820729800\mathrm{E}{-}02$
H	$2.26378061500\mathrm{E}{+}01$	α	$1.16600000000\mathrm{E}{-}05$
I	$6.71675601120\mathrm{E}{+}01$		

BERYLLIUM

c	$7.97500000000\mathrm{E}{-}01$	J	$-2.62045226172\mathrm{E}{+}01$
s	$1.09100000000\mathrm{E}{+}00$	γ	$1.18000000000\mathrm{E}{+}00$
F	$2.07189823068\mathrm{E}{+}00$	c_v	$4.74000000000\mathrm{E}{-}01$
G	$-2.90125259335\mathrm{E}{+}01$	ν_0	$5.34759358000\mathrm{E}{-}01$
H	$-7.55281579097\mathrm{E}{+}01$	α	$1.23300000000\mathrm{E}{-}05$
I	$-7.78921352738\mathrm{E}{+}01$		

LEAD

c	$2.02800000000\mathrm{E}{-}01$	J	$-8.19360638134\mathrm{E}{+}00$
s	$1.51700000000\mathrm{E}{+}00$	γ	$2.03000000000\mathrm{E}{+}00$
F	$-5.36373066032\mathrm{E}{+}01$	c_v	$3.00000000000\mathrm{E}{-}02$
G	$-2.32081021785\mathrm{E}{+}02$	ν_0	$8.81834220000\mathrm{E}{-}02$
H	$-2.09714940297\mathrm{E}{+}02$	α	$2.83700000000\mathrm{E}{-}05$
I	$-7.10476387559\mathrm{E}{+}01$		

REFERENCES

1. W. C. Davis and B. G. Craig, "Smear Camera Technique for Free Surface Velocity Measurement," Rev. Sci. Instrum. 32, 579-581 (1961).

2. W. E. Deal, "Measurement of Chapman-Jouguet Pressure for Explosives," J. Chem. Phys. 27, 796-800 (1957).

3. R. Meyer, Explosives (Verlag Chemie, Weinheim, New York, 1977).

4. K. Hess, Mitt. Art u. Geniewesen 10, 139 (1879).

5. H. Kast, "Die Brisanzbestimmung und die Messung der Detonationsgeschwindigkeit von Sprengstoffen," Zeitschrift für das Gesamte Schiess-und Sprengstoffwesen 8, 88-93 (1913).

6. H. Kast, "Ueber Brisanz und ihre Berechnung," Zeitschrift für das Gesamte Schiess-und Sprengstoffwesen 15, 171-173 (1920).

7. R. Becker, "Zu Theorie der Detonation," Zeitschrift für Elektrochemie 23, 40-49 (1917).

8. R. Becker, "Die Grundgleichungen für Verbrennung und Detonation," Zeitschrift für Tech. Physik 3, 249-256 (1922).

9. C. L. Mader, Numerical Modeling of Detonations (University of California Press, Berkeley, 1979).

10. L. C. Smith, "On Brisance and a Plate Denting Test for the Estimation of Detonation Pressure," Explosivstoffe 5, 106-110 (1967) and 6, 130-134 (1967).

11. A. N. Dremin and P. F. Pokhil, "The Detonation Wave Parameters of Trotyl, Hexogen, Nitroglycerin, and Nitromethane," Doklady Akad. Nauk. SSSR, English transl., Phys. Chem. Sect. 128, 839-841 (1959).

12. P. G. Hoel, Elementary Statistics, 2nd Ed. (John Wiley & Sons, New York, (1966).

13. R. E. Swanson, "One-Dimensional Calculation of Shock-Loaded Polycrystalline Beryllium," Los Alamos Scientific Laboratory report LA-5943-MS (1975).

14. C. L. Mader and M. S. Shaw, "User's Manual for SIN," Los Alamos Scientific Laboratory report LA-7264-M (September 1978).

15. J. D. Kershner and C. L. Mader, "2DE, A Two-Dimensional Continuous Eulerian Hydrodynamic Code for Computing Multicomponent Reactive Hydrodynamic Problems," Los Alamos Scientific Laboratory report LA-4846 (1972).

Page Range	Domestic Price	NTIS Price Code	Page Range	Domestic Price	NTIS Price Code	Page Range	Domestic Price	NTIS Price Code	Page Range	Domestic Price	NTIS Price Code
001-025	$ 5.00	A02	151-175	$11.00	A08	301-325	$17.00	A14	451-475	$23.00	A20
026-050	6.00	A03	176-200	12.00	A09	326-350	18.00	A15	476-500	24.00	A21
051-075	7.00	A04	201-225	13.00	A10	351-375	19.00	A16	501-525	25.00	A22
076-100	8.00	A05	226-250	14.00	A11	376-400	20.00	A17	526-550	26.00	A23
101-125	9.00	A06	251-275	15.00	A12	401-425	21.00	A18	551-575	27.00	A24
126-150	10.00	A07	276-300	16.00	A13	426-450	22.00	A19	576-600	28.00	A25
									601-up	†	A99

†Add $1.00 for each additional 25-page increment or portion thereof from 601 pages up.